DTU Library

Numerical Investigation of Damping of Torsional Beam Vibrations by Viscous Bimoments

Hoffmeyer, David; Høgsberg, Jan Becker

Published in:
Proceedings of the 8th ECCOMAS Thematic Conference on Smart Structures and Materials

Publication date:
2017

Document Version
Peer reviewed version

Link back to DTU Orbit

NUMERICAL INVESTIGATION OF DAMPING OF TORSIONAL BEAM VIBRATIONS BY VISCOUS BIMOMENTS

David Hoffmeyer & Jan Høgsberg

Department of Mechanical Engineering, Technical University of Denmark
Nils Koppels Allé, building 404, DK-2800 Kongens Lyngby, Denmark
e-mail: davhoff@mek.dtu.dk, jhg@mek.dtu.dk, www.dtu.dk

Key words: Torsional beam vibrations, damping, warping, viscous bimoment, complex natural frequency, finite element method.

Abstract. Damping of torsional beam vibrations of slender beam–structures with thin–walled cross–sections is investigated. Analytical results from solving the differential equation gover–ning torsion with viscous bimoments imposed at the boundary, are compared with a numerical approach with three–dimensional, isoparametric elements. The viscous bimoments act on the axial warping displacements associated with inhomogeneous torsion, and are in a numerical for–mat realized by suitable configurations of concentrated, axial forces describing discrete dampers. It is illustrated by an example that significant damping ratios may be obtained for a beam with an open cross–section.

1 INTRODUCTION

Torsional vibrations may be induced in slender, thin–walled beam–structures by e.g. wind, if the loads on the beam act with a certain eccentricity relative to the shear center of the cross-section. For beams with asymmetric cross-sections the elastic and shear centers do not coincide, whereby the flexural and torsional vibrations couple. In both cases the total dynamic response may be damped by damping the torsional motion of the beam. Slender structures like long bridge decks, aircraft wings or wind turbine blades may be prone to aerodynamic instabilities like flutter, where flexural and torsional vibrations couple. Flutter is associated with apparent negative damping that cannot be sufficiently compensated by the inherent structural damping. To avoid flutter and e.g. to reduce fatigue stresses by aerodynamic forces, supplemental damping is therefore required.
Torsional vibrations of thin–walled beams are associated with inhomogeneous torsion which generates out-of-plane, axial warping displacements that are often significant at the boundaries of beams with open cross-sections. The free, torsional vibration characteristics including warping were originally investigated by Gere [1] who solved for the natural frequencies and mode shapes of beams with various boundary conditions, and by Carr [2] where an energy apporach was applied to obtain approximate frequency equations for a few combinations of boundary conditions.

Subsequently Gere and Lin [3] studied the coupling between flexural and torsional vibrations, and the coupling with restrained thin–walled beams by Lin [4]. Numerical results using a finite element approach were compared with analytical results by Mei [5], and Friberg [6] derived an exact dynamic element stiffness matrix, though without the effect of warping. Analytical solutions of frequencies and mode shapes for prismatic beams excited by harmonic, torsional loads have been derived by Augustyn and Kozién [7].

Damping of torsional vibrations has only briefly been addressed in the literature. Narayanan and Malik [8] attached viscoelastic layers to the flanges of a beam with an open cross–section; Jansen and van der Steen [9] considered damping of torsional vibrations in oil well drillstrings; and recently Augustyn and Kozién [10, 11] glued piezoelectric actuators to a beam to reduce the torsional vibrations. Christiano and Salmela [12] showed that the restraining of warping results in an often considerable increase in natural frequency and change in vibration characteristics. This localized effect of restrained warping was utilized to introduce a substantial amount of supplemental damping by Høgsberg et. al. [13], where viscous boundary conditions were applied through pure bimoments at the supports. They solved the eigenvalue problem associated with free vibrations with respect to the complex-valued natural frequency and corresponding damping ratio. They demonstrated that significant damping ratios could be realized by these viscous bimoments at the beam supports.

The present paper performs a numerical investigation of the changed dynamic behaviour of thin-walled beams with applied viscous bimoments at the boundaries. The results in terms of natural frequencies and damping ratios are compared with [13]. The numerical procedure is based on a linear finite element approach with three-dimensional, isoparametric elements. In a simple numerical code, the bimoments are easily represented by concentrated, axial forces distributed over the cross-section. These viscous forces are proportional to the velocity of the given node and are added to the equations of motion by an influence vector describing the points of application. As they are proportional with velocity, they constitute a damping term and result in a modified damping matrix. Setting up the equations of motion in a state-space format yields an eigenvalue problem, from which the corresponding complex natural frequencies and damping ratios are extracted.

2   UNCOUPLED TORSIONAL VIBRATIONS

Consider a beam element of length ℓ, axial coordinate x and transverse axes $\{y, z\}$. The axial displacement is $u(x, y, z, t)$ and the angle of twist is $\theta(x, t)$ as seen in Fig. 1a. In the present analysis it is assumed that flexural and torsional vibrations uncouple because of coinciding elastic centers.

The differential equation governing the torsional vibration problem is set up by energy relations which require the elastic and kinetic energy. The elastic strain energy contains contribution from homogeneous and inhomogeneous torsion, respectively given as

$$U = \int_\ell \tfrac{1}{2} GK(\theta')^2 \, dx + \int_\ell \tfrac{1}{2} EI_\psi(\theta'')^2 \, dx \tag{1}$$

where G is the shear modulus, K is the torsion stiffness parameter, E is Young's modulus and I_ψ is the warping moment of inertia with ψ indicating the sector–coordinate or warping function.
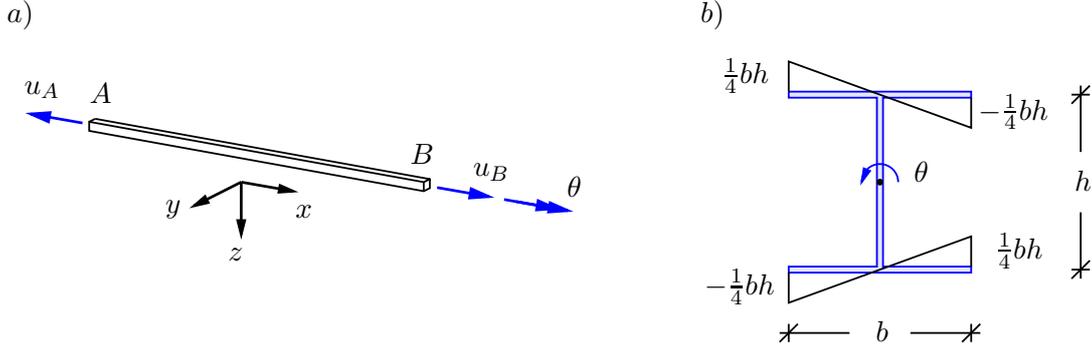
Figure 1: Degrees of freedom and coordinates a) and sector–coordinate ψ for an I–profile with a positive angle of twist b).

For an I–profile the distribution of the sector–coordinate is shown in Fig. 1b. The kinetic energy o the torsional motion is

$$T = \int_\ell \tfrac{1}{2}\,\rho J \dot{\theta}^2 \, dx \tag{2}$$

where ρ is the mass density and J is the polar moment of inertia taking the distribution of the mass into account. Energy dissipation may be defined through a viscous damping coefficient either distributed along the beam by $c_0(x)$ or acting at discrete points via c described by Dirac's delta function δ. As dampers may be applied at discrete points the latter is relevant whereby the dissipated energy D then takes the form:

$$D = \int_\ell c_0(x)\,\dot{\theta}^2 \, dx = \int_\ell c\,\delta(x - x_0)\,\dot{\theta}^2 \, dx \tag{3}$$

where x_0 indicates the point of application of the discrete damper. In the case of damped vibrations the change in mechanical energy is balanced by the dissipated energy, $\dot{U} + \dot{T} = -D$. Performing the differentiation of the energy balance and using integration by parts yields the governing differential equation as

$$EI_\psi \theta'''' - GK\theta'' + \rho J\ddot{\theta} = 0 \tag{4}$$

As no continuous form of damping is intended, the last expression in (3) is instead applied as a boundary condition. Thus, (4) is valid between the points of application of external dampers. A time harmonic solution of the form $\theta = \varphi\,e^{i\omega t}$ may be assumed with ω being the natural frequency and φ the spatial solution. Inserting the frequency solution into (4) and following the approach by Gere [1], the spatial solution may be expressed as

$$\varphi = D_1 \cosh(\alpha x) + D_2 \sinh(\alpha x) + D_3 \cos(\beta x) + D_4 \sin(\beta x) \tag{5}$$

introducing the four integrations constants D_1 to D_4 – determined by the boundary conditions – and the two apparent and real–valued wave numbers defined as

$$\alpha^2 = \sqrt{\tfrac{1}{4}k^4 + \lambda^4} + \tfrac{1}{2}k^2 \quad , \quad \beta^2 = \sqrt{\tfrac{1}{4}k^4 + \lambda^4} - \tfrac{1}{2}k^2 \tag{6}$$

This formulation of the solution introduces the warping length scale k, wave speed v and scaled wave number λ respectively as

$$k^2 = \frac{GK}{EI_\psi} \quad , \quad v^2 = \frac{GK}{\rho J} \quad , \quad \lambda^4 = \left(\frac{k\omega}{v}\right)^2 \tag{7}$$

It is noted that v represents the wave speed for the homogeneous torsion problem. The spatial solution to the torsion problem in terms of the vibration form is obtained from (5) by use of relevant boundary conditions. Applying the boundary conditions yields transcendental equations which must be solved iteratively for the combined set of α and β. One wave number is then given by the other through (6), and the use of the third expression in (7) determines the frequency ω. For more details see e.g. [1, 13].

2.1 Viscous Bimoment at the Boundary

A viscous condition on the boundary may be imposed in several ways. In [13] a viscous normal stress distribution was applied at the beam supports acting through the axial displacement producing a bimoment. This normal stress was distributed across the cross-section of the beam in a continuous manner. In the case of active control a discrete device would produce a concentrated force proportional to the velocity at specific points at the cross-section. A viscous, concentrated force $F_d(y, z, t)$ at the boundary is

$$F_d = \pm c\, \dot{u}_d \tag{8}$$

where c is a viscous damping coefficient and $\dot{u}_d(y, z, t)$ is the axial velocity, positive in the x–direction. The force is defined as positive in tension, whereby the "+" in (8) refers to the left end of the beam at $x = 0$ and the "−" refers to the right end at $x = \ell$. The axial displacement due to torsion is given through the sector–coordinate, and the corresponding velocity is

$$\dot{u}_d = -\psi\, \dot{\theta}_d' \tag{9}$$

see e.g. Vlasov [14]. A series of discrete dampers may be applied at the boundary each dissipating energy. Thus the second expression in (3) indicates a sum of the viscous damping coefficients associated with the given damper and the velocity at that particular point. In combination with (8) the rate of external work D produced by the dampers is formulated as the sum of the contributions of the viscous forces multiplied with the energy conjugate velocity by

$$D = \pm \sum_j F_{d,j}\, \dot{u}_{d,j} = \pm \sum_j c\, \dot{u}_{d,j}^2 = \pm \left(\dot{\theta}_d'\right)^2 \sum_j c\, \psi_j^2 \tag{10}$$

where ψ_j is the sector–coordinate at the location of the j'th damper and c is here assumed to be constant for all dampers. A bimoment as shown in Fig. 2a is usually noted with a double arrow due to the classical example shown in Fig. 2b. Here two opposite bending moments are applied at the flanges. Vectorially they add up to zero, and a pure bimoment is thus a kinematic and not a static condition. It does not generate a resulting force (or moment) but acts as a concentrated change in rotation curvature. The bending moments, however, may be decomposed into force couples as seen in Fig. 2c. A given configuration of concentrated, axial forces therefore generates
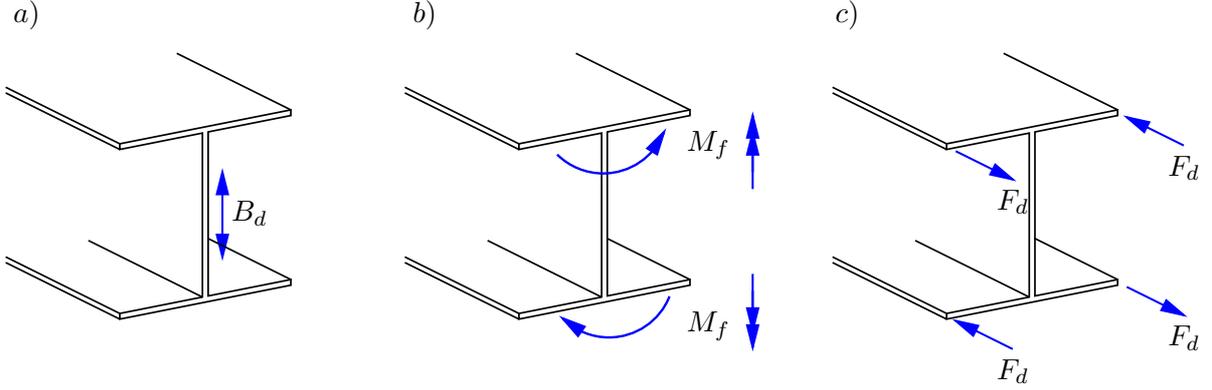
Figure 2: I–profile beam with a bimoment $a)$, bending moments at the flanges generating the bimoment $b)$ and equivalent configuration of concentrated, axial forces $c)$.

a bimoment through the sector–coordinate. By definition the bimoment produces work through the negative gradient of the angle of twist, see e.g. Vlasov [14]. Thus, the rate of work produced by a bimoment is $D = -\dot{\theta}'_d B_d$. Equating this rate of work with (10) yields

$$B_d = \mp \dot{\theta}'_d \sum_j c\,\psi_j^2 \tag{11}$$

The bimoment produced by the dampers $B_d(t)$ must be balanced by the section bimoment at the boundary $B(x,t) = -EI_\psi \theta''(x,t)$. The dynamic boundary condition then takes the form

$$\theta''_d \mp \eta\,\dot{\theta}'_d = 0 \tag{12}$$

with the effective viscous damping parameter $\eta = \sum_j c\,\psi_j^2/EI_\psi$. The form of (12) is identical to [13] with exception of the effective parameter η. Here the viscous damping coefficient c is scaled relative to the amount of dampers, the corresponding sector–coordinates at the points of application and the warping stiffness EI_ψ. Inserting the frequency solution $\theta = \varphi\,\mathrm{e}^{i\omega t}$ yields the harmonic boundary condition

$$\varphi'' \mp i\omega\eta\varphi' = 0 \tag{13}$$

which is directly applicable in connection with the transcendental equations governing the torsional vibration problem.

3 DAMPING OF TORSIONAL VIBRATIONS

When not considering a beam element but modelling the entire structure by a finite element procedure, a discretized, multi–degree–of–freedom system with n degrees of freedom may be assumed. The equations of motion are set up by the elastic, kinetic and dissipated energy. The elastic energy gives the stiffness contribution through the stiffness matrix $\mathbf{K}$, the kinetic energy gives the inertia contribution through the mass matrix $\mathbf{M}$ and the dissipated energy gives the applied, discrete viscous forces as described in (8) and in the second term in (10). The energy balance $\dot{T} + \dot{U} = -D$ then gives

$$\mathbf{M}\ddot{\mathbf{q}}(t) + \mathbf{K}\mathbf{q}(t) = -\mathbf{f}_d(t) \tag{14}$$

where $\mathbf{q}(t)$ is a column vector containing the degrees of freedom and $\mathbf{f}_d(t)$ are the externally applied viscous forces. In this case the inherent structural damping is neglected. Damping may be constituted as a series of dampers modelled as equivalent concentrated, viscous forces acting through a viscous damping coefficient c and the velocity of the corresponding nodes in the discretized system:

$$\mathbf{f}_d(t) = \left(\sum_j^{nd} c_j \mathbf{w}_j \mathbf{w}_j^T \right) \dot{\mathbf{q}}(t) = \widetilde{\mathbf{C}}\dot{\mathbf{q}}(t) \tag{15}$$

Here c_j is the viscous damping coefficient associated with the j'th damper and $\mathbf{w}_j$ is an influence vector describing the points in the structure connected to the damper. The column vector $\mathbf{w}_j$ thus contains 1 at the location of the damper and otherwise 0's. In this case, however, a constant viscous damping coefficient is used for all dampers. Inserting (15) into (14) yields the equations of motion with a modified damping matrix

$$\mathbf{M}\ddot{\mathbf{q}} + \widetilde{\mathbf{C}}\dot{\mathbf{q}} + \mathbf{K}\mathbf{q} = \mathbf{0} \tag{16}$$

These modified equations of motion with damping included yields a quadratic eigenvalue problem. However, they may be formulated in a state–space format

$$\frac{d}{dt}\begin{bmatrix}\mathbf{q}\\\dot{\mathbf{q}}\end{bmatrix} = \begin{bmatrix}\mathbf{0} & \mathbf{I}\\-\mathbf{M}^{-1}\mathbf{K} & -\mathbf{M}^{-1}\widetilde{\mathbf{C}}\end{bmatrix}\begin{bmatrix}\mathbf{q}\\\dot{\mathbf{q}}\end{bmatrix} \tag{17}$$

where $\mathbf{I}$ is a $n \times n$ identity matrix. Assuming a time–dependent, partial solution the state–space format constitutes an ordinary eigenvalue problem, from which the eigenvalue $i\omega$ and corresponding eigenvector may be extracted. For damped vibrations the natural frequency ω is generally complex–valued and usually expressed as

$$\omega = |\omega|\left(\sqrt{1-\zeta^2} + i\zeta\right) \tag{18}$$

with ζ being the damping ratio defined by the imaginary part of the natural frequency

$$\zeta = \frac{\text{Im}[\omega]}{|\omega|} \tag{19}$$

In the complex plane the natural frequency ω constitutes a semicircle between the undamped frequency ω_0 and the corresponding upper limit frequency ω_∞. In the former case the damper(s) have no effect and the viscous damping coefficient therefore is $c = 0$. In the corresponding extreme case where $c \to \infty$ the damper locks and the node, at which the damper is attached, simply becomes restrained against axial movement.

4 EXAMPLE

In the following an example is used to illustrate the theory from Section 2, the numerical procedure established in Section 3 and to illustrate the use of concentrated, axial forces as a measure of damping.
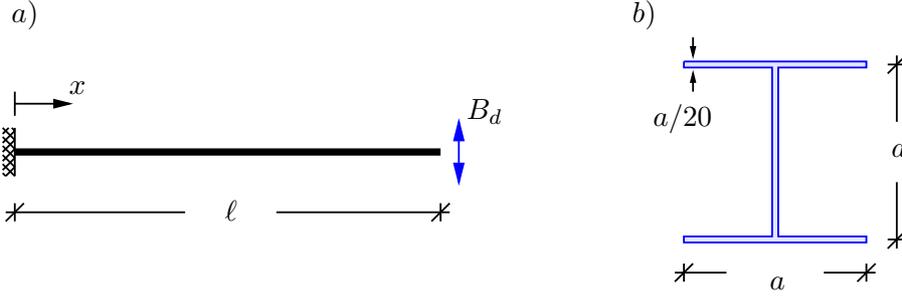
Figure 3: Fixed–free beam with viscous bimoment B_d at $x = \ell$ a) and I–profile cross–section b).

4.1 Damping of a fixed–free beam.

Consider the fixed–free beam in Fig. 3a. The beam has the length ℓ, is fixed at $x = 0$ with restrained rotation and warping and is free at $x = \ell$. The beam cross–section is an open I–profile with height and width a and thickness $t = a/20$, see Fig. 3b. With the chosen cross-section, material and length of the beam the warping length scale normalized with the length of the beam is $k\ell = 3$ and thus represents a slender structure. For a particular viscous bimoment at the boundary at $x = \ell$, the complex natural frequency ω and corresponding damping ratio ζ are obtained by determining the integration constants in (5) by use of the boundary conditions. For the fixed–free beam with damping at $x = \ell$ the boundary conditions are

$$\varphi(0) = 0 \quad , \quad \varphi'(0) = 0 \quad , \quad \varphi''(\ell) + i\omega\eta\varphi'(\ell) = 0 \quad , \quad k^2\varphi'(\ell) - \varphi'''(\ell) = 0 \tag{20}$$

With these homogeneous boundary conditions and the homogeneous differential equation (4) the torsion problem constitutes an eigenvalue problem where the spatial solution (5) leads to a transcendental equation. In [13] it is derived as

$$
\begin{aligned}
&\frac{(\alpha\ell)^4 + (\beta\ell)^4}{(\alpha\ell)^2(\beta\ell)^2} \cosh(\alpha\ell)\cos(\beta\ell) + \frac{(\alpha\ell)^2 + (\beta\ell)^2}{(\alpha\ell)(\beta\ell)} \sinh(\alpha\ell)\sin(\beta\ell) + 2 \\
&+ i\omega\eta\ell \frac{(\alpha\ell)^2 + (\beta\ell)^2}{(\alpha\ell)^2(\beta\ell)^2} \cosh(\alpha\ell)\cos(\beta\ell)\big[\alpha\ell\,\tanh(\alpha\ell) + \beta\ell\,\tan(\beta\ell)\big] = 0
\end{aligned}
\tag{21}
$$

This equation is solved iteratively for $\alpha\ell$ and $\beta\ell$, while the third expression in (7) determines the frequency and by (19) the damping ratio is found. In obtaining a semi–circle in the complex plane, illustrating the variation of the frequency, the viscous damping coefficient c – contained within the effective damping parameter η – is varied in the interval $c \in [0\,;\infty[$. In this example a series of configurations for the distribution of discrete dampers is applied, see. Fig. 4. The first configuration seen in Fig. 4a consists of a single damper applied at one corner of the I–profile, and the resulting warping of the cross–section is thus only partly restrained. The second configuration is a more effective measure of restraining warping as two dampers are located at opposite corners where the largest warping displacements occur, see Fig. 1b. The profile may though still warp, and thus the third configuration is applied which effectively prevents the cross–section from warping almost completely. The two configurations in Figs. 4a and 4b do not constitute pure bimoments as they generate a normal force – and in the first case also
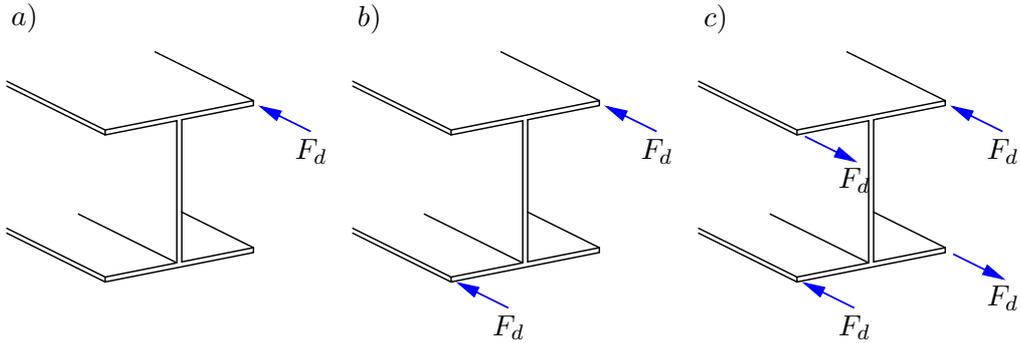
Figure 4: Three configurations of dampers; opposite corners a), all corners b) and distributed along flanges c).

bending moments – which must be accounted for. However, together with the third configuration they serve to illustrate the amount of damping that might by obtained by restraining at the right locations and with a proper number of dampers. The two configurations with non–pure bimoments may even serve to illustrate the possibility of damping coupled flexural vibrations, if the right structural set–up could be established.

The frequency loci and damping ratios for the three different configurations obtained by solving (21) are seen as the solid curves in Figs. 6a and 6b, respectively. By all three configurations of dampers the analytical model yields the same results in terms of undamped frequency ω_0 and the frequency with the dampers being locked ω_∞, corresponding to infinite damping. The dynamic boundary condition (12) restrains warping of the entire cross–section in a unified manner, and does not take the possible modes of warping with the dampers applied into account. The optimal value of the viscous damping parameter c_{opt} is therefore different in the three cases, but plotted as the effective damping parameter η the three sets of curves coincide as seen in Fig. 6b.

Frequencies and damping ratios

In the numerical comparison a standard finite element approach is used with solid, isoparametric elements. A special bi–cubic–linear element is exploited to model thin flanges and a cubic–bi–linear element for connections and corner – these are illustrated in Fig. 5.
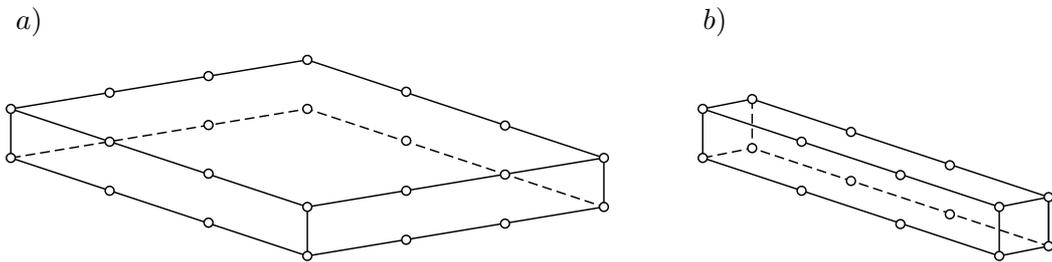

Figure 5: Isoparametric 24–node bi–cubic–linear a) and 16–node cubic–bi–linear b) element.
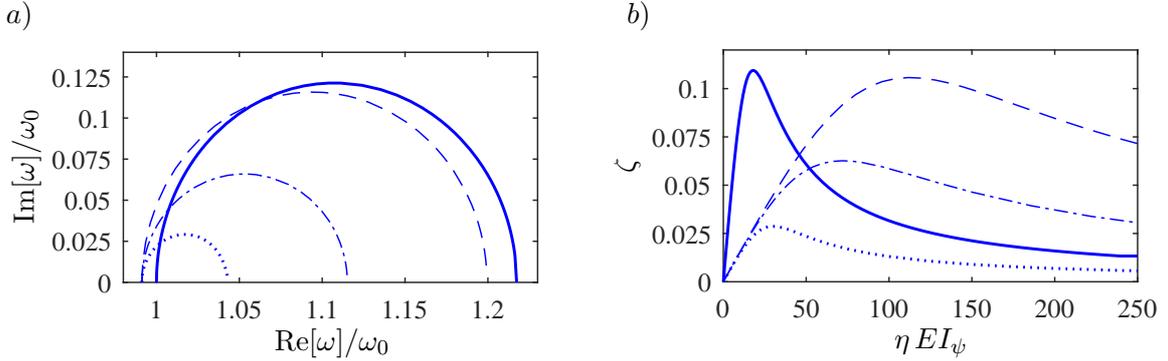
$a)$ $b)$

Figure 6: Frequency loci $a)$ and damping ratios $b)$ showing the results from $(-)$ the analytical procedure and numerical procedure with $(\cdots)$, $(-\cdot-)$ and $(--)$ representing the three bimoment configurations shown in Figs. $4a$, $4b$ and $4c$ respectively.

The elements are intended for modelling of thin-walled beams where a linear interpolation across the thickness is sufficient and a cubic interpolation in the flange–wise direction to capture the parabolic stress variations associated with shear. The I–profile is thus sufficiently modelled with seven elements in the cross–section in the case of a simple static analysis. See e.g. Høgsberg & Krenk [15] for the use of a two–dimensional version of these elements for general cross–sectional analyses of thin–walled beams. In the present case, however, a further discretization of the cross–section is necessary in order to capture the warping effect. As two nodes across the thickness of the flanges are present, a damper at each node of the corners are applied in order to avoid any unnecessary distortion of the cross–section as the damping effect increases. Thus, the damping forces F_d in Fig. 4 constitute a set of two dampers.

Solving the eigenvalue problem in the state–space format for the complex frequency and corresponding damping ratio for the three configurations of dampers yield the frequency loci and distribution of the damping ratio illustrated with the non–solid curves in Fig. 6. As seen the undamped frequency ω_0^{FEM} is 0.9 % lower than the analytical solution. This may be due to the torsional mode in the numerical example not representing 'pure torsion' – as the analytical method requires – but contains some minor distortion, e.g. local deformations of the flanges. The analytical approach is independent of the shape of the cross–section and only works through the cross-sectional parameters, but a three–dimensional numerical model takes this into account. In the case of $c \to \infty$ the boundary condition (12) completely restrains the warping at the free end, and the increment, $(\omega_\infty - \omega_0)/\omega_0$, in the frequency is 0.217 in the analytical case. The numerical model, however, only requires an axial restraining of the nodes at the corners of the I–profile where the dampers are attached. As the largest warping displacements occur at the corners, restraining these will have an essential influence on the warping of the rest of the cross–section. As the cross–sections in the three cases in Fig. 4 still are able to warp locally when $c \to \infty$, the corresponding frequencies ω_∞^{FEM} will be lower compared to the analytical model, which is also seen in Fig 6a. For the configurations shown in Figs. $4a$, $4b$ and $4c$ the increments in frequencies, $(\omega_\infty^{FEM} - \omega_0)/\omega_0$, are 0.043, 0.115 and 0.199 relative to the analytical ω_0, corre-
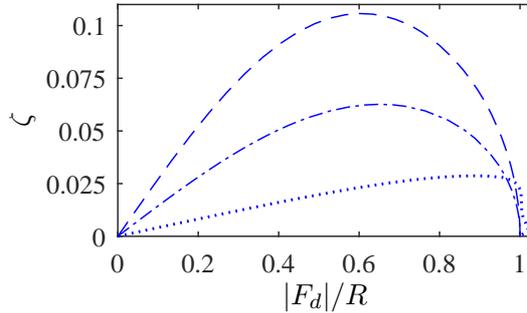
9

Figure 7: Damping ratio given as a function of damper force, for the three damper configurations.

sponding to an increase in stiffness from increased restraining of the warping. The increase in locked frequency has a direct consequence on the damping ratio; the bigger the frequency locus the more damping it is possible to obtain. This is also evident in Fig. 6*b* where the damping ratio ζ increases from 0.029 through 0.063 to 0.106 for the three configurations, compared to 0.109 in the analytical case. This should correspond to approximately half of the frequency increment, but due to ω_0^{FEM} not completely coinciding with ω_0 the values are just slightly off. By this it is noted that the numerical and analytical models match quite well, as the damping ratios are almost identical in the case 4*c* when restraining the entire cross–section.

In this example identical viscous damping coefficients c are used for all dampers. And larger damping ratios may be reached by application of different damping coefficients optimised for each damper. Different cross–sections where warping is more pronounced may equivalently result in even large damping ratios. However, for closed cross–sections associated with larger $k\ell$–values the obtainable damping ratios are limited due to the vanishing warping displacements. In that case an amplified warping displacement may be induced by including a slit along the beam, whereby non–vanishing, relative axial displacements occur.

Damper force

As damping of torsional vibrations by restraining of warping displacements prospectively is intended for beam–structures within civil or mechanical engineering, it is of interest to consider the magnitude of the forces occurring in the dampers. As the eigenvalue problem solved is complex, the force in the damper is also complex. Thus, the magnitude of the force vector for the *j*'th damper is $|F_{d,j}| = |c_j\, \mathbf{w}_j^T\, \dot{\mathbf{q}}|$. Assuming a time dependent solution of the form $\mathbf{q} = \mathbf{q}_0\, e^{i\omega t}$ the force takes the form

$$|F_{d,j}| = |i\, c_j\, \omega\, \mathbf{w}_j^T\, \mathbf{q}_0| \tag{22}$$

This force, however, is scaled according to the corresponding eigenvector and does not represent the actual magnitude. But related to the reaction force R in the case of infinite damping, the relation between the two forces is comparable, provided that the eigenvectors are scaled identically. Fig. 7 shows the damping ratio given as a function of the force of the damper in a single corner of the I–beam, in Fig. 4. For the three configurations in Figs. 4*a*, 4*b* and 4*c* the force ratios $|F_d|/R$ corresponding to maximum damping are 0.887, 0.650 and 0.602 respectively.

10

It is seen that quite large portions of the reaction force must be realized at optimal damping, and for the single damper configuration almost 90 % of the reaction force is present in the damper. This indicates that a configuration of several dampers that effectively restrains warping is most advantageous.

5 CONCLUSION

A previously developed novel method for damping of torsional vibrations of thin–walled beams by control of warping displacements has been investigated and compared with a numerical finite element procedure. The torsional vibrations are damped by restraining the out–of–plane warping displacements by applying viscous bimoments at the boundary of the beam. These viscous bimoments are represented by axial, concentrated forces proportional with the velocity of a given node in the numerical model. By an example it is shown that restraining warping is associated with a significant increase in natural frequency depending on the part of the cross–section being restrained. A proper configuration of dampers results in a considerable amount of supplemental damping for a slender beam-structure, even though all dampers in the present paper are associated with identical viscous damping coefficients. The undamped and infinitely damped natural frequencies are however not exactly identical due to the numerical model taking the actual geometry of the beam into account. This suggests that a final design should be carried out by a numerical procedure to get accurate calibration of the dampers, as well as the forces in the dampers which may be close to the reaction force when locking the damper.

REFERENCES

[1] Gere, J. M., *Torsional vibrations of Beams of Thin–Walled Open Section*, ASME Journal of Applied Mechanics (1954), **21**, pp. 381–387.

[2] Carr, J. B., *The Torsional Vibration of Uniform Thin–Walled Beams of Open Section*, The Aeronautical Journal of the Royal Aeronautical Society (1968), vol. 73, pp. 672–674.

[3] Gere, J. M. & Lin, Y. K., *Coupled Vibrations of Thin–Walled Beams of Open Cross–Section*, ASME Journal of Applied Mechanics (1958), **25**, pp. 373–378.

[4] Lin, Y. K., *Coupled Bending and Torsional Vibrations of Restrained Thin–Walled Beams*, ASME Journal of Applied Mechanics (1960), **27**(4), pp. 739–740.

[5] Mei, C., *Coupled Vibrations of Thin–Walled Beams of Open Section using Finite Element Method*, International Journal of Mechanical Sciences (1970), vol. 12 no. 10.

[6] Friberg, P. O., *Coupled Vibrations of Beams – An Exact Dynamic Element Stiffness Matrix*, International Journal for Numerical Methods in Engineering (1983), vol. 19, pp. 479–493.

[7] Augustyn, E. & Kozień, M. S., *Analytical Solution of Excited Torsional Vibrations of Prismatic Thin–Walled Beams*, Journal of Theoretical and Applied Mechanics (2015), **53** no. 4, pp. 991–1004.

[8] Narayanan, S. & Malik, A. K., *Free Vibrations of Thin–Walled Open Section Beams with Constrained Damping Treatment*, Journal of Sound and Vibration (1981), **74**(3), pp. 429–439.

[9] Jansen, J. D. & van den Steen, L., *Active Damping of Self–Excited Torsional Vibrations in Oil Well Drillstrings*, Journal of Sound and Vibration (1995), **179**(4), pp. 647–668.

[10] Augustyn, E. & Kozień, M. S., *A Study on Possibility to Apply Piezoelectric Actuactors for Active Reduction of Torsional Beams Vibrations*, Acta Physica Polonica (2014), Vol. 125.

[11] Augustyn, E. & Kozień, M. S., *FEM Analysis of Active Reduction of Torsional Vibrations of Clamped–Free Beam by Piezoelectric Elements for Separated Modes*, Archives of Acoustics (2014), Vol. 39 no. 4, pp. 639–644.

[12] Christiano, P. & Salmela, L., *Frequencies of Beams with Elastic Warping Restraint*, Journal of the Structural Division (1971), **97** no. 6, pp. 1835–1840.

[13] Høgsberg, J., Hoffmeyer, D. & Ejlersen, C., *Damping of Torsional Beam Vibrations by Control of Warping Displacement*, Journal of Vibration and Acoustics (2016), vol. 138.

[14] Vlasov, V. Z., *Thin–walled Elastic Beams*, (1961) Israel Program for Scientific Translations, Jerusalem.

[15] Høgsberg, J. & Krenk, S., *Analysis of Moderately Thin–Walled Beam Cross–Sections by Cubic Isoparametric Elements*, Computers and Structures (2014), **134**, pp. 88–101.